Weak Temperature Dependence of Electron Transfer Rates in Fixed-Distance Porphyrin - Quinone Model Systems

ARTICLE *in* JOURNAL OF THE AMERICAN CHEMICAL SOCIETY · OCTOBER 1994

Impact Factor: 12.11 · DOI: 10.1021/ja00100a040

4 AUTHORS, INCLUDING:

Joseph W. Perry
Georgia Institute of Technology
321 PUBLICATIONS **12,050** CITATIONS

SEE PROFILE

James E Hanson
Seton Hall University
31 PUBLICATIONS **235** CITATIONS

SEE PROFILE

Weak Temperature Dependence of Electron Transfer Rates in Fixed-Distance Porphyrin–Quinone Model Systems

Lutfur R. Khundkar,[†,‡] Joseph W. Perry,*[,†] James E. Hanson,[§,⊥] and Peter B. Dervan*[,§]

Contribution from the Jet Propulsion Laboratory, California Institute of Technology, Pasadena, California 91109, and Contribution No. 8939 from the Division of Chemistry and Chemical Engineering, California Institute of Technology, Pasadena, California 91125

Received April 13, 1994[⊗]

Abstract: Electron transfer rate constants of several derivatives of [5-(4′-(4″-(2‴,5‴-benzoquinonyl)bicyclo[2.2.2]-octyl)phenyl)-2,3,7,8,12,13,17,18-octamethylporphyrinato]zinc(II) have been measured as a function of temperature in 2-methyltetrahydrofuran, toluene, and toluene-d_8. The observed temperature dependencies of the electron transfer rate constants are relatively weak in both the polar and nonpolar solvents. Nonexponential ET dynamics are observed at low temperatures and described in terms of an initial (k_{ET}^0) and an average ET rate constant (k_{av}). The k_{ET}^0 values for the molecules with different driving forces, spanning a range of 0.2 eV, show parallel trends over the range of temperatures studied. The trends in k_{ET}^0 are described in terms of the effects of temperature-dependent changes in solvent dielectric constants on the barrier height. Good agreement is observed for the case of toluene solvent, using a semiclassical model, but poorer quantitative agreement is found for the 2-methyltetrahydrofuran data. The temperature dependence of k_{av} is described using a model incorporating an angle-dependent electronic coupling and interconversion of rotational conformers. A temperature-dependent solvent isotope effect is observed on going from toluene to toluene-d_8, with k_{ET}^0(toluene)/k_{ET}^0(toluene-d_8) being as large at 1.5 over the range of temperatures studied.

1. Introduction

Photoinduced electron transfer (ET) in molecular systems has long been of interest in chemistry and biology.[1-6] In recent years, much effort has been directed toward a better understanding of the influence of variables such as driving force, donor–acceptor distance and relative orientation, and solvent properties on ET rates. One impetus for such studies has been the desire to gain greater insight into the mechanisms which lead to efficient charge separation as achieved by photosynthetic reaction centers (RC). Such insights promise to be useful in the design of synthetic biomimetic catalytic systems,[7] photochromic materials,[8] and molecular electronic devices[9] based on photoinduced ET.

Numerous experimental studies have been performed on synthetic model compounds where some of the molecular parameters can be systematically varied in order to elucidate their relative importance.[1c,4] In particular, much attention has been focussed on the driving force ($-\Delta G°$) dependence of ET rates, which has led to the validation[3] of Marcus' prediction of an inverted region.[2a] The temperature dependence of ET in bacterial RCs[10] has been difficult to reconcile with the Marcus ET model which treats the relevant vibrational degrees of freedom classically. These results have been interpreted[10] using a semiclassical model which accounts for quantum vibrational effects. While the classical and semiclassical models both predict an inverted region at high driving forces, they differ in the predicted shape of the ET rate vs driving force function. In the classical model, the predicted dependence for log k_{ET} is parabolic, centered at an optimum value of $-\Delta G°$, and the reaction is strongly activated in both the normal and inverted regions. The semiclassical model predicts an asymmetric dependence, with a more gradual decline in rates in the inverted region, and a broad range of $-\Delta G°$ where the reaction is essentially activationless. This has inspired recent interest in measurements of the temperature dependence of ET rates in model systems.[11]

In our studies of synthetic porphyrin–quinone molecules, we have examined a model system containing a zinc(II) *meso*-phenyloctamethylporphyrin linked to various substituted quinones (generally denoted as ZnPLQ). The porphyrin (donor) and quinone (acceptor) are covalently linked by a rigid, saturated

† Jet Propulsion Laboratory.
‡ Present address: Department of Chemistry, Northeastern University, Boston, MA 02115.
§ Division of Chemistry and Chemical Engineering.
⊥ Present address: Department of Chemistry, Seton Hall University, South Orange, NJ 07079.
⊗ Abstract published in *Advance ACS Abstracts,* September 1, 1994.

(1) (a) Gust, D.; Moore, T. A. *Science* **1989**, *244*, 35. (b) Connolly, J. S.; Bolton, J. R. In *Photoinduced Electron Transfer*; Fox, M. A., Chanon, M., Eds.; Elsevier: New York, 1988. (c) Wasielewski, M. R. *Chem. Rev.* **1992**, *92*, 435.
(2) (a) Marcus, R. A. *J. Chem. Phys.* **1965**, *43*, 679. (b) Marcus, R. A.; Sutin, N. *Biochim. Biophys. Acta* **1985**, *811*, 265. (c) Hopfield, J. J. *Proc. Natl. Acad. Sci. U.S.A.* **1974**, *71*, 3640. (d) Jortner, J. *J. Chem. Phys.* **1976**, *64*, 4860. (e) Sutin, N. *Acc. Chem. Res.* **1982**, *15*, 275.
(3) (a) Miller, J. R.; Calcaterra, L. T.; Closs, G. C. *J. Am. Chem. Soc.* **1984**, *106*, 3047–3049. (b) Gunner, M. R.; Robertson, D. E.; Dutton, P. L. *J. Phys. Chem.* **1986**, *90*, 3783–3795. (c) Wasielewski, M. R.; Niemczyk, M. P.; Svec, E. B.; Pewitt, E. B. *J. Am. Chem. Soc.* **1985**, *107*, 1080. (d) Fox, L. S.; Kozik, M.; Winkler, J. R.; Gray, H.B. *Science* **1990**, *247*, 1069.
(4) (a) Oevering, H.; Paddon-Row, M. N.; Heppener, M.; Oliver, A. M.; Cotsaris, E.; Verhoeven, J.; Hush, N. S. *J. Am. Chem. Soc.* **1987**, *109*, 3258. (b) Closs, G. L.; Calcaterra, L. T.; Green, N. J.; Penfield, K. W.; Miller, J. R. *J. Phys. Chem.* **1986**, *90*, 3673.
(5) (a) McLendon, G. *Acc. Chem. Res.* **1988**, *21*, 160. (b) Closs, G. L.; Miller, J. R. *Science* **1988**, *240*, 440. (c) Siders, P.; Cave, R. J.; Marcus, R. A. *J. Chem. Phys.* **1984**, *81*, 5613. (d) Marcus, R. A.; Siders, P. *J. Phys. Chem.* **1982**, *86*, 622.
(6) (a) Nielson, R. M.; McManis, G. E.; Golovin, M. N.; Weaver, M. J. *J. Phys. Chem.* **1988**, *92*, 3441. (b) McManis, G. E.; Weaver, M. J. *J. Chem. Phys.* **1988**, *90*, 912.
(7) See, e.g.: *Proceedings of 13th DOE Solar Photochemistry Research Conference*; Silver Creek, CO, June 1989.
(8) Beratan, D. N.; Perry, J. W. U.S. Patent 5,062,693, Nov 1991.
(9) Hopfield, J. J.; Onuchic, J. N.; Beratan, D. N. *Science* **1988**, *241*, 817.
(10) (a) DeVault, D.; Chance, B. *Biophys. J.* **1966**, *6*, 825. (b) Kirmaier, C.; Holten, D.; Parson, W. W. *Biochim. Biophys. Acta* **1985**, *810*, 33. (c) Kirmaier, C.; Holten, D.; DeBus, R. J.; Feher, G.; Okamura, M. Y. *Proc. Natl. Acad. Sci. U.S.A.* **1986**, *83*, 957. (d) Gunner, M. R.; Dutton, P. L. *J. Am. Chem. Soc.* **1988**, *111*, 3400.
(11) (a) Harrison, R. J.; Pearce, B.; Beddard, G. S.; Cowan, J. A.; Sanders, J. K. M. *Chem. Phys.* **1987**, *116*, 429. (b) Heitele, H.; Michel-Beyerle, M. E.; Finckh, P. *Chem. Phys. Lett.* **1987**, *138*, 237. (c) Delaney, J. K.; Mauzerall, D. C.; Lindsey, J. S. *J. Am. Chem. Soc.* **1990**, *112*, 957. (d) Liang, N.; Miller, J. R.; Closs, G. L. *J. Am. Chem. Soc.* **1989**, *111*, 8740. (e) Liang, N.; Miller, J. R.; Closs, G. L. *J. Am. Chem. Soc.* **1990**, *112*, 5353. (f) Rodriquez, J.; Kirmaier, C.; Johnson, M. R.; Freisner, R. A.; Holten, D.; Sessler, J. L. *J. Am. Chem. Soc.* **1991**, *113*, 1652. (g) Liu, J.; Bolton, J. R. *J. Phys. Chem.* **1992**, *96*, 1718. (h) Zeng, Y.; Zimmt, M. B. *J. Phys. Chem.* **1992**, *96*, 8395. (i) Kroon, J.; Oevering, H. O.; Verhoeven, J. W.; Warman, J. M.; Oliver, A. M.; Paddon-Row, M. N. *J. Phys. Chem.* **1993**, *97*, 5065. (j) Chen, P.; Mecklenberg, S. L.; Meyer, T. J. *J. Phys. Chem.* **1993**, *97*, 13126.

0002-7863/94/1516-9700$04.50/0

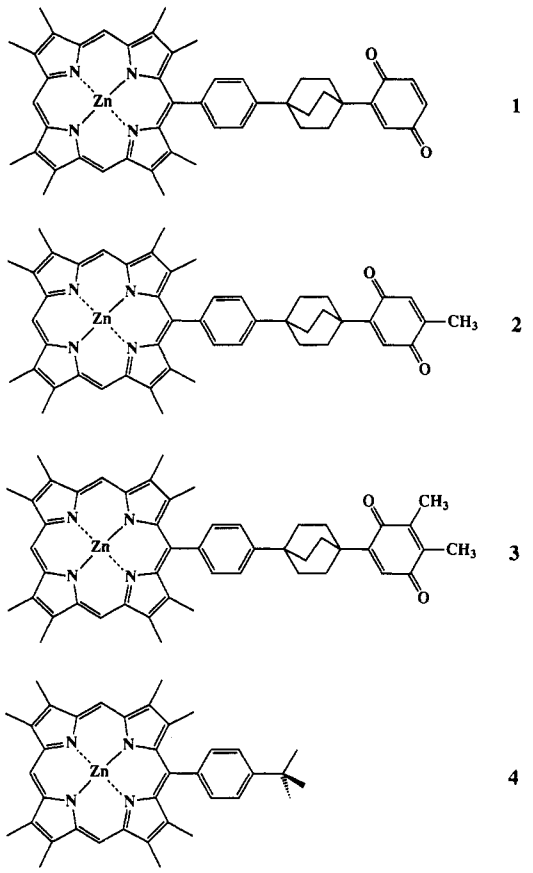

Figure 1. Molecular structures of the zinc(II) *meso*-phenyloctamethylporphyrin[2.2.2]bicyclooctylquinone model compounds.

spacer of [2.2.2]-bicyclooctane units. In addition to its relevance as a model for certain reactions in the photosynthetic RCs, this system offers the advantage of maintaining the donor and acceptor at a fixed distance (14.8 Å center-to-center for molecules with a single spacer) independent of conformational motion. The thermodynamic driving force can be varied by employing substituted quinones, with minimal perturbation of the electronic and nuclear factors involved in ET. Leland *et al.*[12] have previously reported studies of ET in ZnPLQ compounds with different donor–acceptor distances (zero, one, or two spacers) which demonstrated a reduction of the ET rate by a factor of at least 500 for an increase in distance from 14.8 to 18.8 Å. The one-spacer compound was also examined in 2-methyltetrahydrofuran glass at 77 K. The nonexponential decay observed was attributed to a distribution of rotational conformations and an angle-dependent ET rate; the optimal rate was suggested to vary only weakly with temperature. Joran *et al.*[13] reported on the effect of varying driving force at a fixed distance (one spacer) in seven ZnPLQ compounds with substituted quinones. The ET rates were shown to be consistent with either the classical or semiclassical models over the range of driving forces explored (~0.6 eV).

In this paper, we report on the temperature dependence of ET rates, as measured by time-resolved donor fluorescence quenching, in three homologous ZnPLQ compounds in toluene and 2-methyltetrahydrofuran (2MTHF). The ZnPLQ molecules studied, shown in Figure 1, are those where the acceptor is benzoquinone (**1**), methylbenzoquinone (**2**), and dimethylbenzoquinone (**3**), as well as a reference compound with no quinone acceptor, **4**. We find that the rates in both solvents are weakly dependent on temperature, with a decrease in ET rate as the temperature is lowered being observed for the molecules in 2MTHF and an increase in rates in toluene. We also find that the shape of the temperature dependence is quite similar for the different molecules, despite the differences in $\Delta G°$. A semiclassical analysis, which accounts for temperature-dependent changes in solvent dielectric properties, successfully described the trends in toluene, but neither a classical nor a semiclassical treatment gave completely satisfactory results for 2MTHF. The slowing of the average ET rates in 2MTHF at temperatures below 200 K is consistent with an angle-dependent electronic coupling and slow conformational isomerization.

2. Experimental Section

The synthesis of molecules **1–4** has been described previously.[16] Samples were purified by chromatography (CH_2Cl_2, silica gel) immediately prior to the lifetime measurements, and the dichloromethane solvent was removed *invacuo*. 2MTHF was distilled from calcium hydride and stored over calcium hydride under vacuum. Toluene (HPLC grade, Aldrich) and toluene-d_8 (99+ atom %, Aldrich) were used as received (in sealed bottles or ampules, under nitrogen). The appropriate solvent was vacuum transferred onto the sample immediately before the fluorescence measurements. Samples had concentrations between 10^{-5} and 10^{-7} M and were filtered through 0.5 μm filters to minimize light scattering. Absorption spectra were obtained before and after each set of lifetime measurements to verify that the sample had not degraded during the experiment. Special low-temperature cuvettes (1.0 cm path length) with fused edges, obtained from NSG Precision Cells, were used. Cells with glued faces were destroyed whenever the solution froze during a run. Sample temperatures were regulated to within 0.1 K with a liquid helium cooled continuous flow cryostat (Oxford Instruments).[14]

Porphyrin fluorescence decays were measured by time-correlated single photon counting,[15] using a cavity-dumped synchronously mode-locked dye laser (Coherent 702-3) pumped by the frequency doubled output of a CW mode-locked Nd-YAG laser (Quantronix 416). The full width at half maximum of the autocorrelation of the dye laser pulses was typically 5 ps. The wavelength of the exciting light was 570 nm and the fluorescence was collected and passed through a dichroic sheet polarizer set for magic angle detection. Fluorescence at 630 nm was isolated using a cutoff filter (Schott RG610) and a 0.25 m monochromator (Instruments SA, model H-10, 10 nm bandpass) and detected with a MCP-PMT (Hamamatsu 1564U-01). Decays were fit to the sum of two or three exponential components with a nonlinear least-squares method based on the Marquardt algorithm.[16] The instrument response function (typical full width at half maximum 70 ps) was measured using scattered laser light and was accounted for in the fits by iterative reconvolution. The goodness-of-fit was judged according to the reduced χ^2 parameter,[16] of which values in the range of 1.01 to 1.40 were typically obtained and the maximum accepted value was 1.5. In certain cases, as described below, we were unable to obtain good fits to a double exponential model function, in which case a triple exponential function was used.

In a typical set of experiments, the deaerated sample was first equilibrated close to room temperature in the dewar with helium gas flowing continuously. The temperature was lowered slowly, in steps of 10 to 50 K, and the sample allowed to equilibrate for at least 15 min at each temperature before data were acquired. After data had been acquired at the minimum desired temperature for a given run, the sample was warmed slowly, using uniform increments, and data were collected as before. The specific temperatures at which decays were recorded during the warm-up phase were chosen between those used in the cool-down half of the run. The trends of the fitted lifetimes for decays obtained during cooling and warming showed no systematic differences, indicating that the samples were thermally equilibrated at a given temperature when the decays were recorded.

3. Results

ET rates were determined, as described previously,[12,13] by picosecond time-resolved measurements of fluorescence quenching

(12) Leland, B. A.; Joran, A. D.; Felker, P. M.; Hopfield, J. J.; Zewail, A. H.; Dervan, P.B. *J. Phys. Chem.* **1985**, *89*, 5571.
(13) Joran, A. D.; Leland, B. A.; Felker, P. M.; Hopfield, J. J.; Zewail, A. H.; Dervan, P.B. *Nature* **1987**, *327*, 508.
(14) The quoted temperatures are accurate to within ±1 K.
(15) O'Connor, D. V.; Phillips, D. In *Time Correlated Single Photon Counting*, Academic Press: New York, 1984.
(16) (a) Joran A. D.; Leland, B. A.; Geller, G. G.; Hopfield, J. J.; Dervan, P. B. *J. Am. Chem. Soc.* **1984**, *106*, 6090. (b) Joran, A. D. Doctoral Dissertation, California Institute of Technology, Pasadena, CA, 1986. (c) Leland, B. A. Doctoral Dissertation, California Institutue of Technology, Pasadena, CA, 1987.

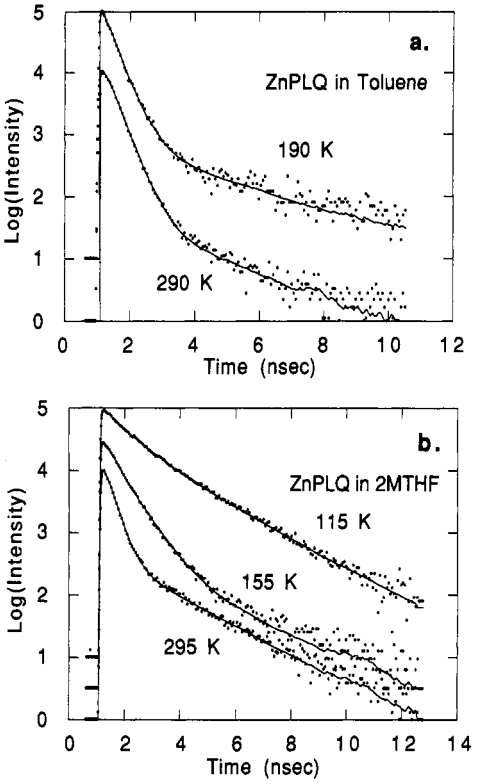

Figure 2. Semilogarithmic plots of typical fluorescence decays of **1** in (a) toluene and (b) 2MTHF at various temperatures. The points are the experimental data, and the solid lines are fitted curves as described in the text. Note that the instrument response function has been accounted for in these fits.

of the excited porphyrin donor. In the absence of an acceptor, the excited porphyrin emits from the S_1 state ($\sim$2.15 eV relative to S_0) with a characteristic lifetime τ_0. In the presence of an acceptor, ET competes with fluorescence and the observed lifetime τ_1 is shortened. The rate constant of electron transfer, k_{ET}, can then be determined as follows:

$$k_{ET} = \frac{1}{\tau_1} - \frac{1}{\tau_0} \tag{1}$$

Representative fluorescence decays are shown in Figure 2 for **1** in toluene and 2MTHF at several different temperatures. The measured fluorescence decays are nonexponential. At room temperature, each decay can be cleanly resolved into two components, the major (>99%) component having a shortened lifetime relative to that of the reference compound **4** due to quenching by intramolecular ET, and the minor component having a lifetime similar to **4** and ascribed to trace amounts of molecules with chemically reduced quinone acceptors.[12] The decays continue to be biexponential as the temperature is lowered until a phase transition (glass or liquid-solid) is approached, where they become more complex (multiexponential). The solvents were fluid over the range of temperatures studied. In toluene and toluene-d_8, the decays showed only a small change over the full range of temperatures studied: room temperature to the freezing point of the solvent ($\sim$180 K). In 2MTHF, the fluorescence decays varied weakly as the temperature was lowered from room temperature to $\sim$180 K. On further cooling (to 110 K), the decays became progressively slower.[17]

The range of temperatures over which the decays could be adequately represented by a sum of two exponentially decaying functions with one of them being dominant depended on the solvent and the particular molecule being studied. Over such a range, the ET rate constant (k_{ET}) is well-defined and was obtained from eq 1, using the decay constant of the fast component as the quenched lifetime. At lower temperatures, where the decays appear multiexponential, a single ET rate for the quenched component cannot be defined. The decays in this temperature range were represented as the sum of three exponentials (eq 2), with the longest component (τ_3) having a lifetime comparable to τ_0. The time-dependent fluorescence intensity, $Q(t)$, was thus taken as

$$Q(t) = \sum_{i=1}^{j} a_i \exp\left(\frac{-t}{\tau_i}\right) \tag{2}$$

where $j = 2$ or 3, a_i is the amplitude, and τ_i is the lifetime of the ith component, as obtained from fits of the model function to the data. We used the multiexponential model function above as a means of simulating the observed nonxponential decays. In this way, we approximated a possibly continuous distribution with a few discreet rate constants. Below we discuss the nonexponential decays in terms of the ET dynamics of a distribution of conformers that have a conformationally dependent ET rate constant. Such a dynamical system can be analytically described with a sum of exponentials, each corresponding to a particular conformer, when interconversion is slow. We approximate a possibly larger number of exponential components with just three, because of a lack of detailed knowledge of the number of conformers and their energetics, as discussed below. There could be other reasons for the observed nonexponential decays, such as the ET rate constants being controlled by solvent relaxation and there being a distribution of solvent relaxation times. We argue below that the time scales for solvent relaxation are too fast to be rate limiting for the systems studied.

To characterize the complex ET dynamics, as revealed by multiexponential decays, we calculated an average ET rate parameter, k_{av}, from the reciprocal of the weighted mean of ET time constants, and an initial average ET rate constant, k_{ET}^0, from the weighted mean of the ET rate constants. These quantities, which are different average measures of the ET dynamics when there is a distribution of intrinsic ET rate constants, are defined in eqs 3a and 3b. The k_{ET}^0 parameter is an average

$$k_{av}^{-1} = \tau_{av} = \frac{\sum_{i=1}^{j} a_i \left(\frac{1}{\tau_i} - \frac{1}{\tau_0}\right)^{-1}}{\sum_{i=1}^{j} a_i} \tag{3a}$$

$$k_{ET}^{0} = \frac{\sum_{i=1}^{j} a_i \left(\frac{1}{\tau_1} - \frac{1}{\tau_0}\right)}{\sum_{i=1}^{j} a_i} \tag{3b}$$

measure of the rate constant for ET at early times. The k_{av} parameter is a measure of the average rate constant for ET at long times, as it is more heavily weighted by the slow decay components.

The values of k_{av} and k_{ET}^0 are listed in Tables 1–3. These values represent the results from two or three independent measurements of the fluorescence decays as a function of temperature. In a few cases, at the lowest temperatures, the parameter a_3 increased significantly above the $\sim$1% level observed at higher temperatures, indicating that a significant fraction of the molecules has an ET rate constant smaller than τ_0^{-1}. In these cases, k_{ET}^0 was calculated using all three exponential components.

(17) In our studies, the solvent was liquid even at the lowest temperature at which results are reported. On further cooling, the solvent usually froze. Decays measured as the solution equilibrated at these low temperatures showed significant lengthening of the decays in toluene and toluene-d_8.

Table 1. Temperature-Dependent ET Rate Constants[a] for **1–4** in Toluene

T (K)	ZnPLQ (1) k_{av}[b]	ZnPLQ (1) k_{ET}^0[c]	ZnPLQMe (2) k_{ET}^0[c]	ZnPLQMe$_2$ (3) k_{ET}^0[c]	ZnPtBu (4) τ_0^{-1}[d]
305		2.4	1.03	0.38	
300		2.5	1.08		
295			1.15	0.40	
290		2.6	1.15	0.40	0.67
285		2.7		0.41	
280			1.22		
270		2.9	1.30	0.45	
265		2.9			
260			1.31	0.47	0.66
250		3.1	1.39	0.51	
240		3.2	1.47	0.54	
235		3.2	1.51	0.54	
225			1.54	0.57	0.65
220		3.3	1.44	0.59	
215			1.63	0.61	
210		3.4	1.65	0.63	
205		3.4	1.69		
200			1.72	0.68	
195	3.2	3.5	1.79	0.70	
190	3.2	3.9	1.75	0.73	
185			1.86		
180	3.2	4.0	1.89	0.83	

[a] $k_{ET}^0 = k_{av}$ where only the k_{ET}^0 value is given. Uncertainty in rate constants is <±5%. [b] Inverse of average time constant ($\times 10^{-9}$ s^{-1}). [c] Initial rate constant ($\times 10^{-9}$ s^{-1}). [d] Fluorescence decay rate constant ($\times 10^{-9}$ s^{-1}), uncertainty <5%.

Table 2. Temperature-Dependent ET Rate Constants[a] for **1–4** in Toluene-d_8

T (K)	ZnPLQ (1) k_{ET}^0[b]	ZnPLQMe (2) k_{ET}^0[b]	ZnPLQMe$_2$ (3) k_{ET}^0[b]	ZnPtBu (4) τ_0^{-1}[c]
305			0.36	
300	2.3	1.17		
298	2.4			
295			0.39	
290	2.5	1.20	0.40	0.67
275	2.7	1.26	0.45	
280		1.27	0.42	
265		1.39		
260	2.8	1.39		0.66
250	2.9	1.47	0.50	
245	3.0	1.45	0.52	
240	3.1	1.51	0.52	
235			0.54	
230	3.1	1.55		0.65
225		1.55		
220	3.1	1.60	0.55	
215		1.63		
210	3.1	1.58	0.57	
200	3.0	1.56	0.57	0.63
195	2.9	1.44	0.56	
190	2.8	1.34	0.55	
185	2.7		0.54	
180	2.3	1.19	0.54	0.63

[a] $k_{ET}^0 = k_{av}$ for the temperatures examined. Uncertainty in rate constants is <±5%. [b] Initial rate constant ($\times 10^{-9}$ s^{-1}). [c] Fluorescence decay rate constant ($\times 10^{-9}$ s^{-1}), uncertainty <5%.

The contribution of the small initial fraction of unquenched fluorescence observed at room temperature was subtracted from the fraction of the component with the longest lifetime at low temperatures. The measured fluorescence lifetimes of reference compound **4** in toluene and toluene-d_8 and compound **1** reduced to the ET inactive hydroquinone form with lithium borohydride in 2MTHF are also listed in Tables 1–3, respectively.[18] The lack of fluorescence quenching in the reduced form of **1** provides strong evidence for ET being the dominant quenching mechanism in the nonreduced forms. The slight increase of these lifetimes with decreasing temperature has been accounted for in calculating k_{ET}^0 and k_{av}.[19]

Table 3. Temperature-Dependent ET Rate Constants[a] for **1–3** and the Reduced Form of **1** in 2MTHF$_4$

	ZnPLQ (1)		ZnPLQMe (2)		ZnPLQMe$_2$ (3)		ZnPLQH$_2$[e]
T (K)	k_{av}[b]	k_{ET}^0[c]	k_{av}[b]	k_{ET}^0[c]	k_{av}[b]	k_{ET}^0[c]	τ_0^{-1}[d]
300		3.2				1.03	
295		3.1		2.1		1.04	0.58
290		3.0				1.05	
280				2.0		1.04	
275		3.0				1.05	0.58
270				2.0			
260		3.0				1.04	
250		3.2				1.05	0.58
240		2.9		2.0		1.03	
225		2.9		1.9		1.02	0.58
215				1.9		1.03	
195		2.7				1.00	
185		2.6				1.0	
180		2.5				1.0	
175		2.5		1.6		1.0	
170				1.5		0.9	0.56
165	2.4	3.0		1.4		0.9	
155	2.2	2.2	1.1	1.2			
150	1.9	2.7	1.0	1.3		0.9	
145	1.9	1.8	0.9	1.1			
140	1.5	2.7	0.7	1.1		0.8	0.55
135	1.4	2.3	0.5	1.1		0.7	
130	0.9	2.8				0.6	
125	0.7	2.1	0.3	0.9			
120			0.9				0.54
115		1.8		0.8	0.3	0.5	

[a] $k_{ET}^0 = k_{av}$ where only the k_{ET}^0 value is given. Uncertainty in rate constants: for $T > 180$ K, <±5%; from 180 K > T > 140 K, <±10%; for $T < 140$ K, <±20%. [b] Inverse of average time constant ($\times 10^{-9}$ s^{-1}). [c] Initial rate constant ($\times 10^{-9}$ s^{-1}). [d] Fluorescence decay rate constant ($\times 10^{-9}$ s^{-1}), uncertainty <5%. [e] Compound **1** reduced with LiBH$_4$ to the ET inactive hydroquinone.

The temperature dependences of the k_{ET}^0 values for compounds **1–3** are shown in Figure 3, parts a (toluene) and b (2MTHF). Previous electrochemical measurements[13] indicate that $-\Delta G°$ for ET is different for each compound. The differences in their room temperature ET rates have been attributed to these differences in $\Delta G°$. The shape of the temperature dependence for all three compounds is very similar in 2MTHF or toluene. However, there are significant differences between the behavior in toluene and in the relatively polar solvent 2MTHF. In toluene, while the overall effect of temperature on the ET rate constant is quite small, the rate constant shows an unexpected increase as the temperature is decreased over the range studied (305–180 K). Over the same range, with toluene-d_8 as the solvent, k_{ET}^0 shows an identical trend to toluene at high temperature but reaches a maximum around 210 K. Below this temperature, the ET rates in toluene-d_8 decrease with decreasing temperature. In 2MTHF, the rates (k_{ET}^0) decrease slightly as the temperature is decreased.

In Figure 4, we compare the temperature dependence of the k_{ET}^0 values and the k_{av} values for **1** in 2MTHF. Two regimes of behavior of k_{av} may be identified: a high temperature range (300–200 K) where it is essentially temperature independent, and a low-temperature range (200–110 K) where it decreases with decreasing temperature. In the high-temperature range, k_{ET}^0 and k_{av} are indistinguishable, whereas in the low-temperature range the latter is significantly smaller. The random errors in these values are largely due to uncertainty in the fitting of the data. It should be noted that when τ_3 is experimentally indistinguishable from τ_0, we cannot define a k_{av} for the electron

(18) (a) Kong, Loach *J. Heterocycl. Chem.* **1980**, *17*, 737. (b) Loach, et al. *Adv. Chem. Ser.* **1981**, *201*, 515.

(19) A fit of τ_0 to a second-order polynomial of temperature was used to interpolate the experimental values of τ_0. τ_0 values measured in toluene and toluene-d_8 were within experimental error and combined together to determine this fit.

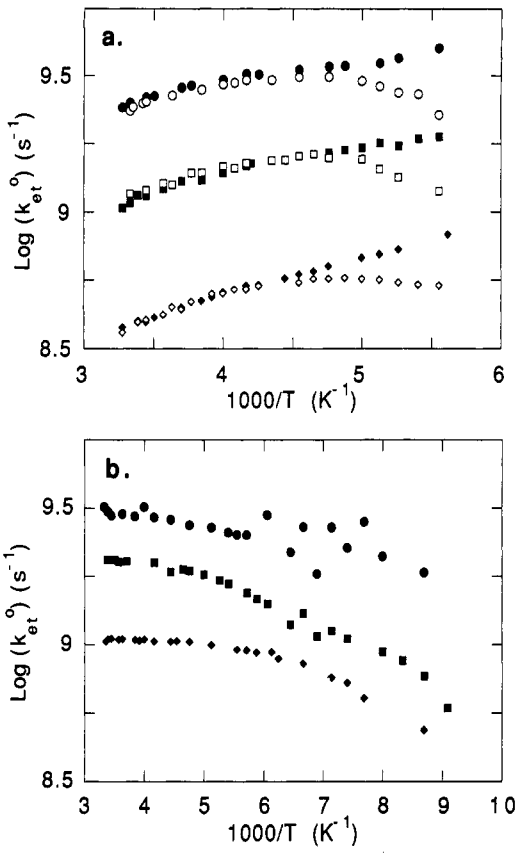

Figure 3. (a) Temperature dependence of initial decay rates for **1** (circle), **2** (square), and **3** (diamond) in toluene (filled symbols) and toluene-d_8 (open symbols). (b) Temperature dependence of initial ET rate constants for ZnPLQ compounds in 2MTHF; symbols as in part a.

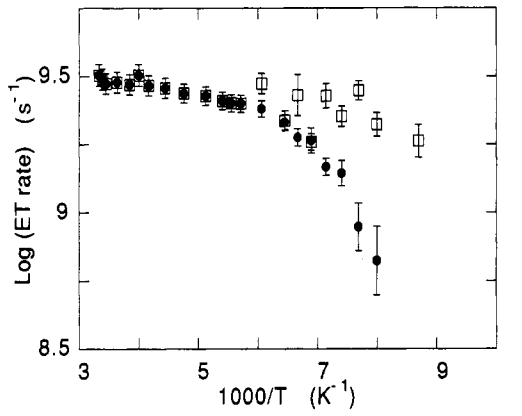

Figure 4. Comparison of temperature dependence of initial (k_{ET}^{0}) and average (k_{av}) ET rate constants for **1** in 2MTHF. The squares are the k_{ET}^{0} values and the circles are the k_{av} values.

transfer process because fluorescence is the dominant channel for decay of the excited state population.

4. Discussion

The classical expression for the rate constant of nonadiabatic electron transfer[2a,b] has the well-known Arrhenius form

$$k_{ET} = \frac{4\pi^2}{h}|H_{RP}|^2\sqrt{4\pi\lambda k_B T}\exp\left(\frac{-(\Delta G^\circ + \lambda)^2}{4\lambda k_B T}\right) \quad (4)$$

where k_B and h are the Boltzmann and Planck constants, T is the temperature, ΔG° is the free energy difference between products and reactants, H_{RP} is the electronic coupling between the donor and the acceptor, and λ is the reorganization energy associated with the electron transfer. The variable λ can be written as the sum of an inner sphere term, λ_i, and an outer sphere term λ_o:

$$\lambda = \lambda_i + \lambda_o \quad (5)$$

The semiclassical expression[2c,d] for the ET rate constant, which results when a single mode of high frequency (ν) is treated quantum mechanically and the low-frequency modes are treated classically, is given by

$$k_{ET} = \frac{4\pi^2}{h}\frac{|H_{RP}|^2}{\sqrt{4\pi\lambda_s k_B T}}\sum_{m=0}^{\infty} e^{-S}S^m/m! \exp\left(\frac{-(\Delta G^\circ + \lambda_s + mh\nu)^2}{4\lambda_s k_B T}\right) \quad (6)$$

ΔG° in this case is the free energy difference between the vibrationless levels of the reactant and product states. λ_v is the reorganization energy of the high-frequency mode, λ_s is the reorganization energy for the classical modes, and S is a distortion parameter defined as $S = \lambda_v/h\nu$. Equation 6 assumes that only the zeroth level of the high-frequency mode is populated in the reactants, i.e. $k_B T \ll h\nu$. At higher temperatures, or for small ν, the total rate is a sum over the contributions of the occupied levels of the reactant. In the limit of high temperature or small ν, the classical and semiclassical equations become equivalent.

The weak, non-Arrhenius temperature dependence observed in the ZnPLQ compounds in both toluene and 2MTHF is contrary to what one would expect from classical ET theory (eq 4). However, since some of the parameters controlling the ET rates are dependent on solvent properties, the observed behavior may be due to the combined effect of these temperature-dependent parameters and the Arrhenius behavior expected of an activated reaction. When the barrier is high, thermal activation plays a dominant role in the reaction dynamics; solvent properties contribute only small corrections. When the barrier is low, changes in solvent properties may dominate the temperature dependence. In the following sections, we attempt to reconcile the observed temperature-dependent ET rates using classical and semiclassical ET expressions, while accounting for the implicit temperature dependence of ΔG° and λ.

4.1. Temperature-Dependent Solvent Properties and ET Rate Constants. One method commonly used to estimate ΔG° in solvents of different polarities is based on the Born expression for solvation energies of ions in a continuous dielectric medium.[20] Neglecting the small stabilization of the nonpolar initial state, the driving force for photoinduced ET in a working solvent can be written as

$$\Delta G^\circ = \Delta G^\circ_{ref} + \frac{e^2}{4\pi\epsilon_0}\left(\frac{1}{\epsilon_s} - \frac{1}{\epsilon_{ref}}\right)\left(\frac{1}{r_{eff}} - \frac{1}{R_c}\right) - \Delta G^\circ_{S_1} \quad (7)$$

where ΔG°_{ref} is the driving force in a reference solvent of static dielectric constant ϵ_{ref}. The static dielectric constant of the working solvent is ϵ_s. The average ionic radius of the two product ions is r_{eff},[21] and the center-to-center distance between donor and acceptor (R_c) is 14.8 Å in our molecules. The last term, $\Delta G^\circ_{S_1}$,

(20) Weller, A. *Z. Phys. Chem. NF* **1982**, *133*, 93.

(21) More accurately, $1/r_{eff}$ is the electrostatic divergence integral for the charge distribution corresponding to the two non-interacting product ions. The assumption that the ions are spherical is invoked when r_{eff} is estimated from molecular structure data.

(22) Schmidt, J. A.; Liu, J. Y.; Bolton, J. R.; Archer, M. D.; Gadzepko, V. P. Y. *J. Chem. Soc., Faraday Trans. 1* **1989**, *85*, 1027.

(23) With ϵ_s set equal to 1, and the term involving R_c ignored, the calculated driving force should be the sum of the adiabatic ionization potential of the donor and the electron affinity of the acceptor in a vacuum. The calculated value of 5.3 eV is indeed in good agreement with estimates of these gas-phase values (Weast, R. C. Ed. *Handbook of Chemistry and Physics*, 60th ed.; CRC Press: Boca Raton, FL, 1982).

Table 4. Solvent Dielectric Parameters, $\Delta G°$ and λ, for 1 in Several Solvents

solvent	$\Delta G°$ [a] (eV)	ϵ_s	ϵ_{op}	$\Delta G°$ [b] (eV)	λ_o [c] (eV)
benzene	−0.67	2.284	2.244	−0.29	0.014
toluene		2.391	2.241	−0.33	0.05
2MTHF	−0.93	6.98	1.977	−0.82	0.65
acetonitrile	−1.01	37.5	1.801	−1.01	0.95

[a] From ref 12, determined from electrochemical measurements. [b] Calculated using eq 7, with acetonitrile as the reference solvent. [c] Calculated using eq 8.

is the transition energy of the lowest excited electronic state of the metalloporphyrin (2.15 eV).

The solvent dependence of the reorganization energy is due mainly to the outer sphere term, which is

$$\lambda_o = \frac{e^2}{4\pi\epsilon_0}\left(\frac{1}{\epsilon_{op}} - \frac{1}{\epsilon_s}\right)\left(\frac{1}{r_{eff}} - \frac{1}{R_c}\right) \qquad (8)$$

where ϵ_{op} is the high-frequency dielectric constant of the working solvent. The dielectric constants, ϵ_{op} and ϵ_s, of a solvent can change significantly with temperature. Consequently, both the driving force and the reorganization energy, and hence the barrier height, can change with temperature.[25] Estimates of these changes in λ_o and $\Delta G°$ can be made if ϵ_s and ϵ_{op} are known as functions of temperature.

In order to make explicit calculations of the temperature-dependent ET rates, we need values for a number of model parameters: H_{RP}, λ_s, λ_v, and ν. We fit the earlier room temperature results, i.e., the solvent and driving force dependent ET rate constants for the series of ZnPLQ molecules of Joran *et al.*,[13] to obtain a consistent set of values of H_{RP}, λ_v, and ν. We chose acetonitrile as the reference solvent and the driving force for **1** in acetonitrile, measured electrochemically, as $\Delta G°_{ref}$. Using r_{eff} = 5.12 Å, as estimated by Schmidt *et al.*[22] for an amide bridged tetraphenylporphyrin quinone compound, we calculated $\Delta G°$ and λ_o for **1** in 2MTHF, toluene, and benzene.[23] These values are collected in Table 4. The $\Delta G°$ values for the various ZnPLQ molecules of ref 13 were obtained using the oxidation potentials of the different substituted quinones.[12,13] In Figure 5, we plot the ET rate constants (from ref 13 and this work) as a function of driving force for the ZnPLQ model compounds in the solvents listed above. To generate this plot we used eq 7 to estimate the absolute driving force for each compound. By using eqs 4 and 6, the corresponding classical and semiclassical rate constants were calculated with use of the following parameters: H_{RP} = 3.5 cm^{-1}, $h\nu$ = 0.12 eV, and λ_v = 0.3 eV. The reorganization energy of the classical modes, λ_s, was taken to be the sum of the contributions from the solvent (λ_o) and the low-frequency intramolecular modes (0.2 eV). As seen in Figure 5, the model calculations give a reasonable description[24] of the room temperature solvent dependence of the ET rate constants for molecules of varying driving force.

The ET rate constants for **1–3** in toluene and 2MTHF at different temperatures were calculated using literature data or estimates of ϵ_s and ϵ_{op} values at corresponding temperatures. Temperature-dependent ϵ_s data for toluene[26] and 2MTHF[27,28]

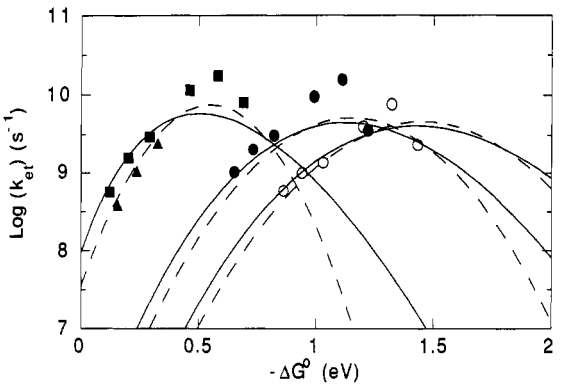

Figure 5. Driving force dependence of ET rate constants for ZnPLQ model compounds in various solvents at room temperature (293 K). The symbols show experimental rate constants from ref 13 and this work in the following solvents: benzene (squares), toluene (triangles), 2MTHF (filled circles), and acetonitrile (open circles). The calculated classical (dashed lines) and semiclassical (solid lines) rate constants for these compounds were obtained using the parameters given in the text.

are available in the literature. We estimated ϵ_{op} for the solvents using the Lorenz–Lorentz expression[29] for the molar refractivity, ρ, which is

$$\rho = \left(\frac{\epsilon_{op} - 1}{\epsilon_{op} + 2}\right)\frac{M}{d} \qquad (9)$$

where M is the molecular weight and d is the density. ρ is considered to be independent of temperature. The ϵ_{op} values of toluene and 2MTHF at different temperature were estimated using the known values at room temperature and the temperature-dependent densities.[30]

4.2. Temperature Dependence of the ET Rate Constants. Before proceeding to the comparison of the model calculations with the experimental results, it is worthwhile to discuss some qualitative features of the observed trends. While a single ET rate constant can be readily obtained near room temperature, the observation of complicated decays at low temperatures indicates a distribution of rate constants. This could be the result of a distribution of "sites" with differing rate constants and slow interconversion between them. Such behavior has been observed in studies of mutant bacterial RCs.[31] We describe the nonexponential dynamics observed in our studies at low temperatures by using two rate constants, k_{ET}^0 and k_{av} (defined earlier). In our experiments, the sample is at thermal equilibrium before the reaction is initiated. Therefore, k_{ET}^0, the apparent initial rate constant, is an average decay constant for an equilibrium (thermal) population distribution. k_{av} is the reciprocal of the average ET time constant, which can reflect changes in the distribution of rate constants if thermally equilibrated populations are not maintained at all times during the reaction. If dynamical averaging between "sites" is fast, thermal equilibrium is maintained at all times and k_{ET}^0 is equal to k_{av}. This is the situation observed above 180 K in 2MTHF and 200 K in toluene. The value of k_{ET}^0, as we calculate it, is not, in principle, very sensitive to the time evolution of the distribution of rates toward slower

(24) It should be noted that these parameters do not constitute a unique set. Several different combinations can yield rates which are in good agreement with the data. However, we were able to identify some constraints on their range, e.g. the total reorganization energy is ca. λ_o + 0.5 eV and the frequency ν is less than ca. 0.15 eV (1200 cm^{-1}).

(25) Temperature-dependent barrier heights as a consequence of temperature-dependent solvent polarity have been shown to be important in charge transfer in other compounds. Hicks, J.; Vandersall, M.; Eisenthal, K. B.; Balarogic, Z. *Chem. Phys. Lett.* **1985**, *116*, 18.

(26) Landolt-Borstein Tables: Physical Constants for Molecules, Part II/6.

(27) (a) Furutsuka, T.; Imura, T.; Kojima, T.; Kawabe, K. *Osaka Univ. Eng. Rep.* **1974**, *24*, 367. (b) Miller, J. R. Private communication.

(28) The ϵ_s values of toluene were available at discrete intervals from ~210 to >320 K. The measurements for 2MTHF were done at 1 kHz (ref 27a) and the equation given there was used over the full range of temperatures in this study, although it is quoted to be accurate above 140 K. The possible errors introduced by these extrapolations are not significant for our conclusions.

(29) Bottcher and Bordewick In *Theory of Dielectric Polarization*; Elsevier, North Holland: Amsterdam, 1986; Vol. 2, Chapter 8 .

(30) (a) Reid, R. C.; Prausnitz, J. M.; Poling, B. E. In *The Properties of Gases and Liquids*, 4th ed.; McGraw-Hill: New York, 1987; p 468. (b) Engler, B. P.; Harrah, L.A. *Sandia Rep.* **1978**, No. 78-1414. As the temperature-dependent density of 2MTHF was only available to 210 K, the function was extrapolated to lower temperatures.

(31) Jia, Y.; DiMagno, T. J.; Chan, C.-K.; Wang, Z.; Du, M.; Hanson, D. K.; Schiffer, M.; Norris, J. R.; Fleming, G. R.; Popov, M. S. *J. Phys. Chem.* **1993**, *97*, 13180.

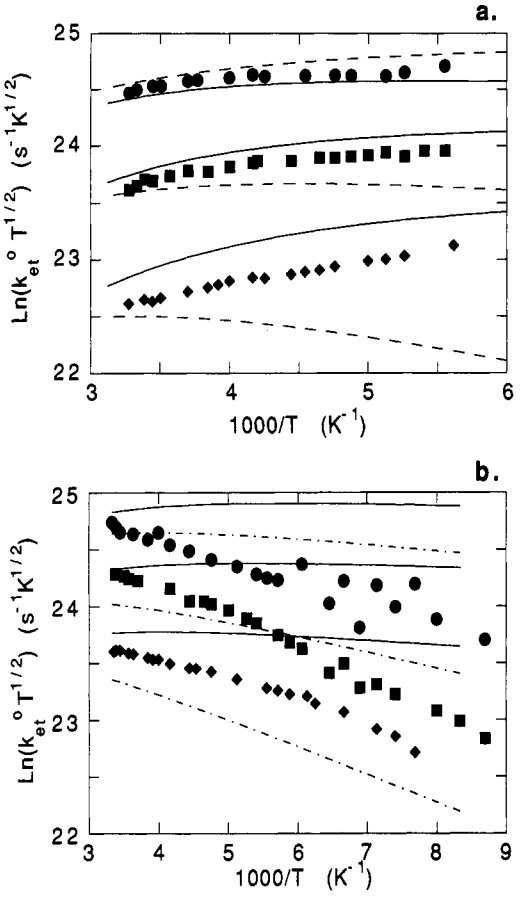

Figure 6. Comparison of experimental temperature dependence of the ET rate constants (k_{ET}^0) with calculated classical (dashed lines) and semiclassical (solid lines) dependences for **1–3** (circles, squares and diamonds, respectively) in (a) toluene and (b) 2MTHF. $|H_{RP}|^2$ was adjusted for each solvent such that the calculated semiclassical rate constant of **1** agreed with the measured value at room temperature. Note that k_{ET}^0 has been multiplied by $T^{1/2}$ to account for the temperature dependence of the preexponential factor.

rates, since it is more heavily weighted by the fast decay components.[32] At lower temperatures, where thermal equilibration between different reactant sites or states may be slow, k_{av} is smaller than k_{ET}^0. To compare intrinsic ET rates over the full range of temperatures studied, we utilize the k_{ET}^0 values. In both 2MTHF and toluene, the various molecules show "parallel" trends in the temperature-dependent behavior of k_{ET}^0. Given the difference in $\Delta G°$ of about 0.2 eV between **1** and **3**, sizable differences between the trends of the three molecules would be expected, to the extent that the barrier height changes due to this difference. The increase of k_{ET}^0 with decreasing temperature observed in toluene for each molecule implies a decrease in barrier height with decreasing temperature. The trends observed for k_{ET}^0 are essentially independent of the change in driving force due to acceptor strength variations but show a clear dependence on solvent and temperature. This indicates that the initial rates are largely controlled by temperature-dependent solvent dielectric constants, which affect the barrier height.

Temperature-dependent ET rates for compounds **1–3** in toluene, calculated using the classical and semiclassical models (eqs 4 and 6), are shown in Figure 6a along with experimental initial rates. Similar calculations for compounds **1–3** in 2MTHF are shown in Figure 6b. The weak temperature dependence of the rates for all three compounds in either solvent indicates a small barrier to ET, consistent with the idea that the driving forces in these ZnPLQ compounds are close to optimal for thermal ET from the S_1 state.

(32) (a) Sumi, H.; Marcus, R. A. *J. Chem. Phys.* **1986**, *84*, 4894. (b) Nadler, W.; Marcus, R. A. *J. Chem. Phys.* **1987**, *86*, 3906.

The classical model predicts activationless behavior only close to the optimal value of $-\Delta G°$, with an increase in the activation energy as $-\Delta G°$ deviates from this value. The semiclassical model predicts activationless behavior over a broader range of $-\Delta G°$. For toluene solvent, the semiclassical model adequately describes the trends, but the classical model does not fit all three compounds as well. For 2MTHF solvent, neither model fits the data well; however, the semiclassical model does show the parallel trends for the different molecules. On the other hand, the apparent activation energy is somewhat closer to that predicted by the classical model. The significance of this is not clear, since a small adjustment of $\Delta G°$ for the molecules in 2MTHF leads to better agreement between our data and the semiclassical model calculations. We have also performed calculations with different combinations of ν and λ and find that as long as these parameters are chosen to give good agreement with the room temperature rates in different solvents, the trends in the temperature dependence of k_{ET}^0 are similar to what is seen in Figure 6. Extensive manipulation of the model parameters to fit the observed temperature dependences was outside the spirit of our modeling effort. More importantly, the success of the model in describing the toluene results suggests that our description of the temperature dependence of the dielectric constants of 2MTHF may have been inadequate. Additionally, 2MTHF may have a specific interaction[29,33] with ZnPLQ molecules that was not accounted for in the model.

4.3. Conformational Isomerization and Nonexponential ET Dynamics. Nonexponential fluorescence decays observed previously for **1** in 2MTHF glass at 77 K were attributed to a distribution of conformers and a conformer-dependent ET rate.[12] The electronic coupling, H_{RP}, should be constant for different solvents or for different quinone substitutions, but it may be quite sensitive to changes in the relative orientation of the porphyrin and quinone.[12,16] Liu and Bolton have invoked a temperature-dependent H_{RP} in a series of porphyrin–amide–quinone molecules to account for changes in donor–acceptor distance (R_c) resulting from conformational flexibility. R_c is fixed in the ZnPLQ molecules here and thus cannot account for a temperature dependence in H_{RP}. A simple model based on orbital overlap results in a dependence of H_{RP} on the dihedral angle θ between the porphyrin and quinone planes, with $H_{RP} \propto \cos\theta$.[34] In ref 12, a uniform distribution over all θ was assumed and used to fit the decays observed in frozen 2MTHF. While such a distribution may be reasonable for a system where molecules undergoing free internal rotation are quickly quenched, our system is better described in terms of temperature-dependent interconversions of stable conformers.

Molecular mechanics (MM2)[35] studies of phenyl bicyclooctyl quinone indicate that two independent internal rotations are relevant. One is rotation about the bond connecting the phenyl ring to the bicyclooctane linker (PB), the other is rotation about

(33) Gutmann, V. *Electrochim. Acta* **1976**, *21*, 661.

(34) A $\cos 2\theta$ dependence on the dihedral angle has been observed for the electronic coupling between two porphyrin rings (Helms, A.; Heiler, D.; McLendon, G. *J. Am. Chem. Soc.* **1991**, *113*, 4325). We believe that a simple p-orbital overlap describes the through-bond interaction between the zinc-porphyrin and quinone in the ZnPLQ molecules (see ref 36) resulting in a $\cos\theta$ dependence.

(35) MM2 calculations were done using PCMODEL (version 4) from Serena Software, implemented on a 80386 class personal computer. The energy was obtained by holding the dihedral angle fixed while minimizing the energy with respect to the remaining degrees of freedom. No significant differences were observed in the barrier height when methyl substitution(s) on the quinone was used.

(36) Electron tunneling matrix elements have been calculated previously for this particular system (Beratan, D. N. *J. Am. Chem. Soc.* **1986**, *108*, 4321). The same assumptions (one orbital overlap and nearest neighbor interactions only) can be used to show that if the s-bonds of the spacer are involved, the orientation of the saturated linker with respect to the donor p-orbital does not affect H_{RP}. Through-bond coupling has also been noted in other porphyrin–quinone systems linked by a long, rigid, saturated bridge (Antolovich, M.; Keyte, P. J.; Oliver, A. M.; Paddon-Row, M. N.; Kroon, J.; Verhoeven, J. W.; Jonker, S. A.; Warman, J. M. *J. Phys. Chem.* **1991**, *95*, 1933).

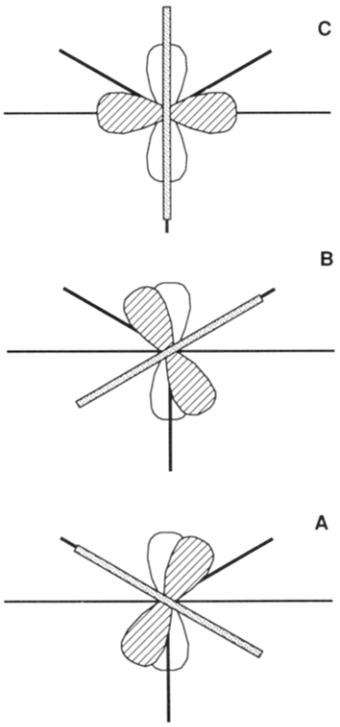

Figure 7. A pictorial representation of the rotational conformers of the ZnPLQ compounds as viewed along the 3-fold symmetry axis of the bicyclooctyl spacer. The horizontal line represents the plane of the porphyrin ring, the shaded box represents the plane of the quinone ring, and the bicyclooctyl spacer is shown as three heavy solid lines pointing away from the center. The unfilled p-orbital represents a p-orbital on the porphyrin donor and the shaded p-orbital represents one on the quinone acceptor.

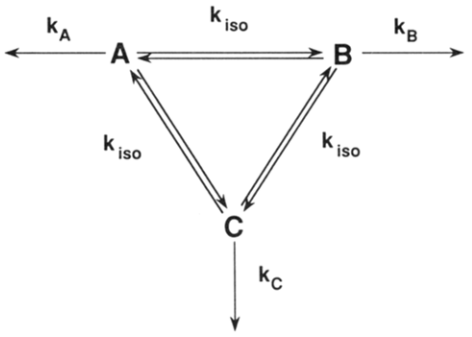

Figure 8. A kinetic scheme for isomerization and electron transfer in the ZnPLQ compounds. k_A, k_B, and k_C are the ET rate constants from the different conformers. k_{iso} is the isomerization rate.

the quinone–bicyclooctane bond (QB). PB rotation is 6-fold symmetric, QB rotation is 3-fold symmetric with two distinct minima. The barrier to rotation about the PB bond is approximately 1 kcal/mol, while the barriers to rotation about QB are between 1 and 2 kcal/mol. These conformers all have the phenyl ring perpendicular to the porphyrin ring, with the bicyclooctane in an eclipsed conformation with both the phenyl ring and the quinone (Figure 7). The conformations differ in the relative orientations (θ) of the planes of the porphyrin and quinone (Figure 8). Compared to a conformation where the porphyrin and quinone are coplanar, the relative magnitudes of H_{RP}^2 for conformers A, B, and C are 0.75, 0.75, and 0.[36] This model therefore predicts that two of these conformers (A and B) should have the same ET rate, and the third conformer should be essentially ET inactive. This three-state model (Figure 8) can be simplified to a two-state model, since the rates of isomerization between conformers are equal and two of them have the same ET rate.

Solution of the rate equations for the two-state model predicts a biexponential fluorescence decay for this system, the two decay constants being functions of the ET and isomerization rates. A specific solution requires three inputs: the ET rates of conformers A (k_A) and C (k_C) and the isomerization rate k_{iso}. We take k_C to be zero since the electronic coupling for C was estimated to be zero. Thus only k_A and k_{iso} need to be specified. $k_A(T)$ can be estimated from the experimentally determined k_{ET}^0 (eq 10).

$$k_{ET}^0 = {}^2/_3 k_A \tag{10}$$

As discussed above, k_{ET}^0 is independent of k_{iso} at any temperature. The factor of $^2/_3$ is a result of only two of the three distinct conformers being ET active. We used a second-order polynomial fit of ln k_{ET}^0 vs $1/T$ to obtain k_A at a given temperature. The conformational isomerization is itself an activated process and its rate was modeled by the high viscosity limit form of Kramer's theory[37]

$$k_{iso} = \frac{AT}{\eta} e^{-E_a/k_B T} \tag{11}$$

The temperature dependence of k_{iso} was calculated by using experimental viscosities (extrapolated from 200 to 120 K) and a barrier height (E_a) of 1 kcal/mol as estimated above. The value of the pre-exponential factor, A, was chosen to obtain agreement between the observed and calculated k_{av} values for **1** in 2MTHF. This results in a room temperature k_{iso} of 5×10^{11} s^{-1}, consistent with NMR measurements[38] on phenylbicyclooctane that yield an internal rotation rate of $\sim 10^{11}$ rad/s at room temperature.

By using the values of k_{iso} determined for **1** and the appropriate k_{ET}^0 values, we calculated k_{av} for compounds **2** and **3** in 2MTHF. These results are shown in Figure 9a, along with the experimental values of $k_{av}(T)$. The agreement between calculated and observed average rates in 2MTHF is quite reasonable. $k_{av}(T)$ was also calculated for toluene, assuming E_a and A are independent of solvent (Figure 9b). These results indicate that isomerization is of minor importance in limiting ET rates in toluene over this temperature range.

Solvent relaxation may also play a role in the nonexponential ET dynamics observed here. To the extent that solvent motion is slow, the ET rate may be controlled by the dynamics of solvent reorientation.[39,40] A characteristic solvation time relevant for ET is the longitudinal relaxation time, τ_L, $\tau_L = (\epsilon_{op}/\epsilon_s)\tau_D$, where τ_D is the Debye relaxation time. Rempel *et al.*[41] have recently reported ET rates for a tetraphenylporphyrin linked to a quinone molecule by an ether linkage. They observe a temperature dependence similar to our results in 2MTHF and suggest that slow solvent dielectric relaxation may be responsible for the change in apparent activation energy near 200 K. Given the flexibility of this bridge, it would not be surprising if internal rotation was also important in their system. By using $\tau_L = 1.5$ ps for 2MTHF at room temperature and temperature-dependent viscosities, we estimate a τ_L value of 70 ps at 120 K. Since ET in **1**–**3** occurs on a much longer time scale even at such low temperatures, we believe that solvent relaxation is not the rate limiting process over the temperature range investigated. This point must be tempered

(37) (a) Kramers, H. A. *Physika* **1940**, *7*, 284–304. (b) Hanggi, P. *J. Stat. Phys.* **1986**, *42*, 105. (b) This also assumes a Stokes–Einstein relation for the relevant friction term. At the simplistic level of this model, this assumption is adequate.

(38) Craik, D. J.; Adcock, W.; Levy, G. C. *Magn. Reson. Chem.* **1986**, *24*, 783–791.

(39) (a) Maroncelli, M.; MacInnnes, J.; Fleming, G. R. *Science* **1989**, *243*, 1674. (b) Kosower, E. M.; Huppert, D. *Annu. Rev. Phys. Chem.* **1988**, *92*, 6495. (c) Onuchic, J.N.; Wolynes, P. G. *J. Phys. Chem.* **1988**, *92*, 6495. (d) Frauenfelder, H.; Wolynes, P.G. *Science* **1985**, *229*, 337. (e) Berne, J. B.; Borkovec, M.; Straub, J. E. *J. Phys. Chem.* **1988**, *92*, 3711.

(40) See, e.g.: Weaver, M. *Chem. Rev.* **1992**, *92*, 463.

(41) Rempel, U.; von Maltzan, B.; von Borczyskowski, C. *Z. Phys. Chem.* **1991**, *170*, 107.

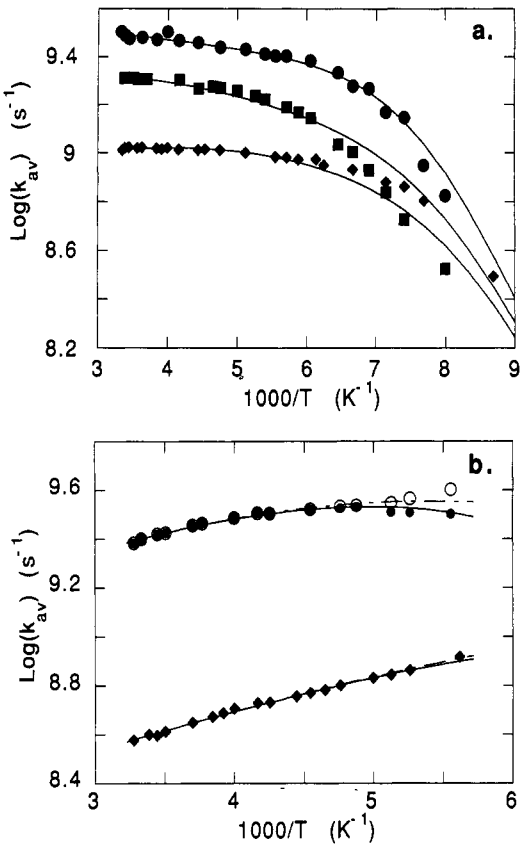

Figure 9. Comparison of the temperature dependence of k_{av} for **1–3** (circles, squares, and diamonds, respectively) in (a) 2MTHF and (b) toluene with that calculated by using the isomerization modulated electron transfer model described in the text. In part b, the open circles are the experimental k_{ET}^0 values. The dashed lines represents a fit to these points and the solid lines represent the calculated k_{av}.

by the lack of direct measurements of τ_L in 2MTHF at different temperatures.

Gaines *et al.*[42] have suggested that in a system where polar solvation contributes significantly to the driving force for photoinduced charge separation, repopulation of the excited singlet state by back transfer may become significant in a frozen solvent (due to reduction of this stabilization energy) and result in biphasic fluorescence decays. Warman *et al.*[43] have discussed a sigmoidal temperature dependence of the lifetime of a charge transfer state in a similar context. We believe that repopulation of the S_1 state by back transfer is not the cause of the nonexponential decays observed in our system at low temperature. As indicated by the fast ET rate in toluene, the charge-separated states in the ZnPLQ molecules in a polarizable solvent such as toluene are at a lower energy than the S_1 state. Given the fact that the solvents are fluid at all temperatures used in our studies, the energy of the charge-separated state should be lower in the more polar solvent, 2MTHF. This would suggest that the barrier to back transfer is larger in 2MTHF than in toluene. In contrast, we observe a greater fraction of long component in 2MTHF as the temperature is lowered.

4.4. Temperature-Dependent Solvent Isotope Effect. As illustrated in Figure 3b, k_{ET}^0 values for **1–3** in toluene-d_8 deviate from those in toluene-h_8 below 210 K, with the rates becoming slower in the deuterated solvent as the temperature is reduced. This isotope effect leads to a ratio of rate constants $k_{ET}^0(h_8)/k_{ET}^0(d_8)$ of $\approx$1.5 at 180 K, the lowest temperature studied. It should be noted that the observed dynamics in toluene-d_8 appear monoexponential, indicating that isomerization is faster than ET in these systems and does not affect the observed dynamics. Furthermore, the rotational reorientation time obtained from NMR and Raman studies[44] is about 50 ps for toluene and slightly longer for toluene-d_8 at 190 K, which is close to the freezing point. Thus changes in orientational relaxation time due to an increase in the moment of inertia on deuteration are not large enough to explain the observed turnover. It is possible that a change in the barrier height due to differences in the temperature-dependent dielectric constants of toluene and toluene-d_8 may be responsible for the observed effects. Due to a lack of adequate data on $\epsilon_s(T)$ and $\epsilon_{op}(T)$, we cannot presently assess this possibility.

4.5. Comparison with Results of Related Studies. The observations of this study bear relevance to studies of ET in other systems. Of particular interest are studies of isolated bacterial photosynthetic RCs and some synthetic model ET systems. Weak temperature dependence of ET rates has been observed for the reaction center protein in *R. sphaeroides* as well as for excited porphyrin to quinone ET in model systems.

Gunner and Dutton[10c] performed an extensive study of ET from bacteriopheophytin to the quinone acceptor in *R. sphaeroides* R26 as a function of $-\Delta G°$, by replacement of the native quinone with a variety of substituted quinones, as a function of temperature. The weak temperature dependence observed over a broad range of driving force demonstrated the importance of nuclear tunneling in this reaction and was accounted for by using a frequency of 120 cm^{-1} for the quantized vibrational mode. This work nicely illustrates the advantage of combined $\Delta G°$ and temperature-dependence studies: such an approach imposes stringent limits on acceptable model parameters and can provide information on the frequencies of the vibrational modes coupled to ET and the reorganization energies.

Delaney *et al.*[11] reported the temperature dependence of excited singlet porphyrin to quinone ET rates in a cofacial zinc–porphyrin cage molecule in several solvents. While the existence of two slowly interconverting conformers complicated the kinetic analysis, weak temperature dependence was observed for one conformer. Both increasing and decreasing rates were observed with decreasing temperature in different solvents. These observations were also attributed to nonadiabatic nuclear tunneling involving high-frequency modes. The small apparent activation energies of varying sign were ascribed to the effect of medium-frequency modes ($\sim$200 cm^{-1}) in addition to the high-frequency ones. The effect of a temperature-dependent barrier was not discussed by these authors.

In contrast, Liang *et al.*[11d] have recently shown that for a model system with very low driving force, and therefore a large barrier, the ET rate is strongly activated. Intramolecular ET from a biphenylyl radical anion to a naphthyl group was investigated as a function of temperature in 2MTHF. Their previous investigation of the $-\Delta G°$ dependence was described by using low-frequency classical modes and a single average high-frequency mode ($\sim$1500 cm^{-1}).[3a] The biphenylyl/naphthyl system was at such low driving force that even the semiclassical model predicts a strong temperature dependence, as observed. It may be noted that in this study, the authors assumed that the driving force for the charge shift reaction was essentially independent of temperature. By use of parameters estimated from the $-\Delta G°$ dependence of ET rates at room temperature and a temperature dependence of λ resulting from changes in solvent dielectric constants, they obtained good agreement between calculated and observed temperature-dependent ET rate constants. Liang *et al.*[11e] have

(42) Warman, J. M.; Smit, K. J.; Jonker, S. A.; Verhoeven, J. W.; Oevering, H. O.; Kroon, J.; Paddon-Row, M. N.; Oliver, A. M. *Chem. Phys.* **1993**, *170*, 359.

(43) Rates of ET from bacteriopheophytin to quinone in RCs in D_2O were found to be different than the corresponding rates in H_2O. In this case, proton–deuteron exchange in the donor could significantly affect the energetics and hence the rate of transfer. Such an exchange is not possible in our metalloporphyrin donor. Examples of solvent isotope effects have also been noted in studies of nonradiative energy transfer (see, e.g., ref 11j).

(44) (a) Spiess, H. W.; Schweitzer, D.; Haeberlen, U. *J. Magn. Reson.* **1973**, *9*, 444. (b) Levy, C.; D'Arrigo, G. *Mol. Phys.* **1983**, *50*, 917.

also found that systems in the inverted region exhibit essentially activationless behavior. Similar results on photoinduced ET have also been observed by other workers.[11i,j]

Harrison *et al.*[11a] have measured temperature-dependent charge separation and recombination rates for linked metalloporphyrin–pyromellitimide molecules in different solvents. They observed fast charge separation which exhibited the same activation energy as the solvent Debye relaxation time. In contrast, the ZnPLQ compounds studied here show weakly activated rates which do not follow the temperature dependence of τ_D and are significantly longer than estimates from the simple scaling law $\tau_D \propto \eta/T$. In the model system of Harrison *et al.*, the distance between donor and acceptor (and hence H_{RP}) may vary with temperature since the bridge is flexible. Such an argument was used by Bolton and co-workers to explain their results on a flexible porphyrin–amide–quinone system.[11g] In the ZnPLQ molecules, the donor–acceptor distance is constant, precluding variations in H_{RP} due to changes in R_c.

5. Conclusions

We have investigated the temperature dependence of ET rates in three ZnPLQ compounds spanning a range of $\Delta G°$ of $\sim$0.2 eV, 0.2–0.4 eV less than the optimal driving force. In this range of driving force, the temperature dependencies are weak and the different compounds show similar trends in each solvent studied. The major features of the temperature dependence of the ET rates in these model compounds can be described by a semiclassical model that includes changes in solvent dielectric constants, for electron transfer coupled to a single high frequency molecular mode ($\sim$1000 cm^{-1}) and low-frequency molecular and solvent modes, but the data do not exclude the classical model conclusively. Our modeling of the effect of the temperature-dependent dielectric constants on the barrier height in 2MTHF overestimates the change in barrier height with temperature. This may result from an inadequate estimate of the temperature-dependent refractive index or from specific interactions which could also affect the barrier height. A second activated process that modulated the rate of electron transfer was observed and interpreted by use of a conformational model in which the ET rate is taken to be a function of the dihedral angle between the porphyrin and quinone planes. This model, which utilized a torsional barrier of 1 kcal/mol, successfully described the temperature dependence of the "average" ET rates constants in both 2MTHF and toluene.

Acknowledgment. This work was performed in part at the Jet Propulsion Laboratory (JPL), California Institute of Technology, and was supported in part by the Department of Energy through an agreement with the National Aeronautics and Space Administration (NASA). P.B.D. and J.E.H. thank the National Science Foundation for financial support. Additional support from the Director's Discretionary Fund at JPL is gratefully acknowledged. L.R.K. thanks NASA and the National Research Council for a Resident Research Associateship at JPL and Dr. John Miller (Argonne National Laboratories) for providing us with data on temperature-dependent dielectric constants and densities of 2MTHF. We thank Profs. David Beratan, Jose Onuchic, John Hopfield, and Rudy Marcus for many helpful discussions.